Model Predictive Control of Thermal Comfort and Indoor Air Quality in Livestock Stable

Zhuang Wu and Murali R. Rajamani and James B. Rawlings and Jakob Stoustrup

Abstract— **In this paper, the implementation of a Model Predictive Control (MPC) strategy for livestock ventilation systems and the associated indoor climate through variable valve opening and exhaust fan, is presented. The design is based on Thermal Comfort (TC) and Indoor Air Quality (IAQ) parameters for poultry in barns. The dynamic models describing the nonlinear behavior of ventilation and associated indoor climate, by applying a so-called conceptual multi-zone method are used for prediction of indoor horizontal variation of temperature and carbon dioxide concentration. The simulation results illustrate the significant potential of MPC in dealing with nonlinearities, handling constraints and performing offset free tracking for multiple control objectives. The entire control systems are able to determine the demand ventilation rate and airflow pattern, optimize the Thermal Comfort, Indoor Air Quality and energy use.**

I. INTRODUCTION

An optimum livestock indoor climate should enhance voluntary feed intake and minimize thermal stresses that affect animals. The alleviation of thermal strain and the maintenance of comfort environment significantly depend on the measurement and control of the air temperature and the humidity. The humidity control is not considered in this work because it has little effect on thermal comfort sensation at or near comfortable temperatures unless it is extremely low or high. On the other hand, proper indoor air quality is imperative to maintain the health and productivity of farm workers and animals. Hence, the concentration of contaminant gases, such as carbon dioxide, has to be controlled through the ventilation systems.

Hybrid ventilation systems combine the natural ventilation and mechanical ventilation, and have been widely used for livestock. Most existing control systems used for livestock barns are based on analysis with the single zone method, which assumes that the indoor air temperature and contaminant concentration are uniform [1]. However, the actual indoor environment at any controlling sensors (especially when the sensors are located horizontally) will depend on the air flow distribution that is usually depicted as a map of the dominant air paths. Therefore, the control system for large scale livestock barns neglecting the horizontal variations could obviously result in significant deviations from the optimal environment for the sensitive pigs or poultry. Furthermore, the performance of currently used control schemes for livestock are limited when large disturbances occur in the presence of input saturation.

As stated in books [2], [3] and papers [16], [5], [6], Model Predictive Control (MPC) has become the advanced control strategy of choice by industry mainly for the economically important, large-scale, multi-variable processes in the plant. The rationale for MPC in these applications is that it can deal with strong non-linearities, handle constraints and modeling errors, fulfill offset-free tracking, and it is easy to tune and implement.

In this paper, the livestock indoor environment and its control system will be regarded as a feedback loop in which the predictive controller provide the optimal actions to the actuators taking into account the significant disturbances and random noises. The MPC strategy is not only expected to give good regulation of the horizontal variation of temperature and concentration, but also to minimize the energy consumption involved with operating the valves and the fans.

II. PROCESS DYNAMIC MODELING

A. Modeling of Thermal Comfort and Indoor Air Quality

The schematic diagram of a large scale livestock barn equipped with hybrid ventilation system analyzed with the conceptual multi-zone method is shown in Fig. 1(1), Fig. 1(2) and Fig. 1(3). The system consists of evenly distributed exhaust units mounted in the ridge of the roof and fresh air inlet openings installed on the walls. From the view of direction A and B, Fig. 1(a) and Fig. 1(b) provide a description of the dominant air flow map of the building including the airflow interaction between each conceptual zone. Through the inlet system, the incoming fresh cold air mixes with indoor warm air and circulates via the exhaust system, and then drop down to the animal environmental zones slowly in order to satisfy the zonal comfort requirement.

By applying a conceptual multi-zone method, the building will be divided into several macroscopic homogeneous conceptual zones horizontally so that the nonlinear differential equation relating the zonal temperature and zonal concentration can be derived based on the energy and mass balance equation for each zone as (1) and (2). The subscript i denotes the zone number.

$$M_i c_{p,i} \frac{dT_i}{dt} = \dot{Q}_{i+1,i} + \dot{Q}_{i,i+1} + \dot{Q}_{in,i} + \dot{Q}_{out,i} + \dot{Q}_{conve,i} + \dot{Q}_{source,i}, \quad (1)$$

Z. Wu is with Department of Electronic Systems, Aalborg University, Aalborg, DK 9220, Denmark zhuangwu@es.aau.dk

M. R. Rajamani is with Department of Chemical and Biological Engineering, University of Wisconsin-Madison, Madison, WI 53706, U.S.A. rmurali@wisc.edu

J. B. Rawlings is with Department of Chemical and Biological Engineering, University of Wisconsin-Madison, Madison, WI 53706, U.S.A. rawlings@engr.wisc.edu

J. Stoustrup is with Department of Electronic Systems, Aalborg University, Aalborg, DK 9220, Denmark jakob@es.aau.dk

ISBN: 978-960-89028-5-5

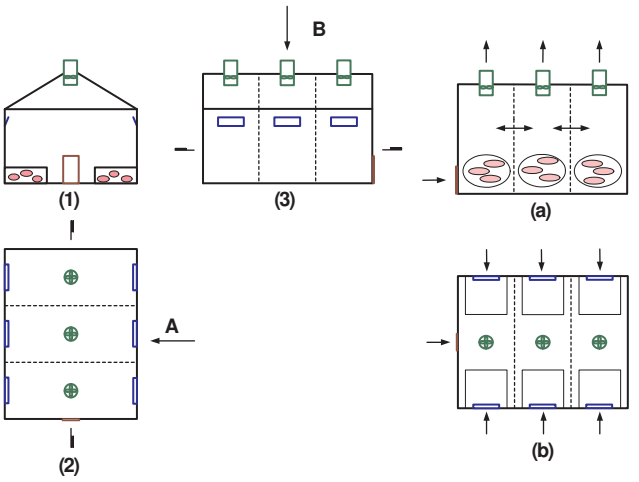

Fig. 1. Synoptic of Large Scale Livestock Barn and the Dominant Airflow Map of the Barn

$$\frac{dC_{r,i}}{dt} = C_{r,i+1}\cdot\dot{n}_{i+1,i} + C_{r,i}\cdot\dot{n}_{i,i+1} + C_{r,i}\cdot\dot{n}_{out} + C_{r,o}\cdot\dot{n}_{in} + \frac{G_i}{V_i}\cdot \tag{2}$$

For (1), T_i is the indoor zonal air temperature (^oC), $c_{p,i}$ is the specific heat of the air ($J\cdot kg^{-1}\cdot K^{-1}$), M_i is the mass of the air (kg), $\dot{Q}_{i+1,i}$ and $\dot{Q}_{i,i+1}$ indicate the heat exchange (J/s) due to the air flow across the conceptual boundary of zone i and zone $i+1$, while for the middle zones which have heat exchange with neighbor zones on each side, two more parts $\dot{Q}_{i-1,i}$, $\dot{Q}_{i,i-1}$ will be added. $\dot{Q}_{in,i}$, $\dot{Q}_{out,i}$ represent the heat transfer (J/s) by mass flow through the inlet and outlet respectively. The convective heat loss through the building envelope is denoted by $\dot{Q}_{conve,i}$ (J/s) and described as $U\cdot A_{wall,i}\cdot(T_i - T_o)$, where U is the heat transfer coefficient, and A_{wall} is the area of the wall. The heat source of the zone $\dot{Q}_{source,i}$ includes the animal heat productivity and heat dissipated from heating system.

For (2), the rate of concentration is indicated as $C_{r,i}\cdot\dot{n}_i$, in which $C_{r,i}$ (m^3/m^3) represents the zonal concentration and $\dot{n}_i$ (h^{-1}) is the air exchange rate. The rate of the animal carbon dioxide generation denoted by G_i ($10^{-3}m^3/h$) is approximately 12 times the actual activity level denoted by M_a (l/h), which is measured in *met* as stated in (3). The zonal volume is V_i (m^3).

$$G = 12\cdot M_a. \tag{3}$$

B. Modeling of Inlet Vent and Exhaust Fan System

The inlet system provides variable airflow directions and controls the amount of incoming fresh air by adjusting the bottom hanged flaps. The volume flow rate through the inlet is calculated by (4), where C_d is the discharge coefficient, A is the geometrical opening area (m^2), ΔP (Pa) is the pressure difference across the opening and can be computed by a set of routines solving thermal buoyancy and wind effect as (5). V_{ref} stands for the wind speed at reference height. C_P is the wind induced pressure coefficient and its value changes according to the wind direction, the building surface orientation and the topography and roughness of the terrain in the wind direction. The subscript NPL stands for the Neutral Pressure Level. The coefficient C_d for the inlet system, varies considerably with the inlet type, opening area, as well as incoming air temperature and flow rate. However, for simplifying the computation, we use a constant value of this coefficient for all openings, even though it might lead to over/under-prediction of airflow capacity and thereby larger openings than necessary.

$$q_{in} = C_d\cdot A\cdot\sqrt{\frac{2\cdot\Delta P}{\rho}}, \tag{4}$$

$$\Delta P = \frac{1}{2}C_P\rho_o V_{ref}^2 - P_i + \rho_o g\frac{T_i - T_o}{T_i}(H_{NPL} - H_{in}). \tag{5}$$

In the exhaust unit, the airflow capacity is controlled by adjusting the r.p.m. of the fan impeller and by means of the shutter. We introduce a fan law, as a relationship between the total pressure difference ΔP_{fan}, volume flow rate q_{out} and supplied voltage V_{volt} with a specific shutter opening angle which can be approximated in a nonlinear static equation (6), where the parameters a_0, a_1, a_1 are empirically determined from experiments made by SKOV A/S in Denmark. As shown in (7), the total pressure difference across the fan is the difference between the wind pressure on the roof and the internal pressure at the entrance of the fan which considers the pressure distribution calculated upon the internal pressure at reference height denoted by P_i.

$$\Delta P_{fan} = a_0\cdot(V_{volt})^2 + a_1\cdot q_{out}\cdot(V_{volt}) + a_2\cdot q_{out}^2, \tag{6}$$

$$\Delta P_{fan} = \frac{1}{2}\rho_o C_{P,r}V_{ref}^2 - P_i - \rho_i g\frac{T_i - T_o}{T_o}(H_{NPL} - H_{fan}). \tag{7}$$

For a detailed description for developing the models and significant dynamic parameters estimation, we refer to [7].

III. MODEL PREDICTIVE CONTROL

Model Predictive Control (MPC) refers to a class of control algorithms that compute a sequence of manipulated variable adjustments by utilizing a process model to optimize forecasts of process behavior based on a linear or quadratic open-loop performance objective, subject to equality or inequality constraints over a future time horizon.

A. Model Transformation

We regard the livestock ventilation system as two parts by noting that the overall system consists of a static air distribution system (inlet-exhaust air flow system) and a dynamic environmental system (thermal comfort and indoor air quality). Both of these two systems are mildly nonlinear Multiple Input and Multiple Output (MIMO) systems. However, representing or approximating a nonlinear model's dynamic response with some form of linear dynamics is an easy and illuminating way to analyze and solve online optimization, and especially, for processes maintained at nominal operating conditions and subject to small disturbances, the potential improvement of using a nonlinear

model in MPC would appear small. Therefore, the developed nonlinear process models are transformed into a series of Linear Time Invariant (LTI) state space models through linearization around the equilibrium points corresponding to different inter-zonal airflow direction. The Thermal Neutral Zone (TNZ) [8], [9], and the demand concentration level are selected to be the criterion that represent the control objective. Fig. 2 shows the synoptic of the entire system model and the climate control variables.

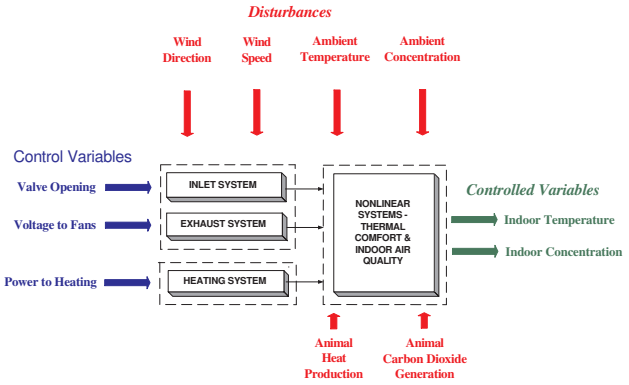

Fig. 2. Synoptic of Entire System Model and Climate Control Variables

Let the nonlinear continuous time model (1) which is represented with three coupled equations for thermal comfort be described in the discrete time linearized dynamics state space form as (8):

$$x_T(k+1) = A_T \cdot x_T(k) + B_T \cdot q(k) + B_{Td} \cdot d_T(k), \quad (8a)$$
$$y_T(k) = C_T \cdot x_T(k) + D_T \cdot q(k) + D_{Td} \cdot d_T(k), \quad (8b)$$

where, $A_T \in \mathbb{R}^{3\times3}$, $B_T \in \mathbb{R}^{3\times9}$, $B_{Td} \in \mathbb{R}^{3\times8}$, $C_T \in \mathbb{R}^{3\times3}$, $D_T \in \mathbb{R}^{3\times9}$, $D_{Td} \in \mathbb{R}^{3\times8}$ are the coefficient matrices with subscript T denoting the model for the thermal comfort system. k is the current sample number. In the similar procedure, we could derive the state space form for the indoor air quality system as (9) according to (2):

$$x_C(k+1) = A_C \cdot x_C(k) + B_C \cdot q(k) + B_{Cd} \cdot d_C(k), \quad (9a)$$
$$y_C(k) = C_C \cdot x_C(k) + D_C \cdot q(k) + D_{Cd} \cdot d_C(k), \quad (9b)$$

where, $A_C \in \mathbb{R}^{3\times3}$, $B_C \in \mathbb{R}^{3\times9}$, $B_{Cd} \in \mathbb{R}^{3\times12}$, $C_T \in \mathbb{R}^{3\times3}$, $D_T \in \mathbb{R}^{3\times9}$, $D_{Td} \in \mathbb{R}^{3\times12}$ are the coefficient matrices with subscript C denoting the model for the concentration system.

By applying the conservation of mass for the livestock building with one single zone concept (10), and through linearization of air flow model deducted through (4) to (7), we can derive the static equation (11).

$$\sum_{i=1}^{6} q_{in}(k) \cdot \rho_o - \sum_{j=1}^{3} q_{out}(k) \cdot \rho_i = 0, \quad (10)$$

$$E \cdot v(k) + F \cdot u(k) + G \cdot w(k) + K \cdot x_T(k) = 0, \quad (11)$$

where, E,F,G,K are coefficients matrices. The definition of $v \in \mathbb{R}^{9+1}$ is: $[q_{in,m}, q_{out,n}, P_i]^T$, $m = 1\cdots6$, $n = 1\cdots3$, where, $[q]^T_{1\times9}$ is a airflow input vector which combines the actuators' signals u and the thermal process controlled variables x_T and x_C.

Connecting and coupling of the airflow model (11) with the environmental models (8) and (9), evolve a finalized LTI state space model representing the entire knowledge of the performances for thermal comfort and indoor air quality around the equilibrium point. The combined process model is shown in (12)

$$x(k+1) = A \cdot x(k) + B \cdot u(k) + B_d \cdot \begin{bmatrix} d_{umd}(k) \\ d_{md}(k) \end{bmatrix}, \quad (12a)$$
$$y(k) = C \cdot x(k) + D \cdot u(k) + D_d \cdot \begin{bmatrix} d_{umd}(k) \\ d_{md}(k) \end{bmatrix}, \quad (12b)$$

where, $A \in \mathbb{R}^{6\times6}$, $B \in \mathbb{R}^{6\times9}$, $C \in \mathbb{R}^{6\times6}$, $D \in \mathbb{R}^{6\times9}$, $B_d \in \mathbb{R}^{6\times12}$, $D_d \in \mathbb{R}^{6\times12}$ are the coefficient matrices. The disturbance transient matrices B_d and D_d are formulated as (13) corresponding to the unmeasured and measured disturbances.

$$B_d = \begin{bmatrix} B_{dumd} & B_{dmd} \end{bmatrix}, D_d = \begin{bmatrix} D_{dumd} & D_{dmd} \end{bmatrix}. \quad (13)$$

x, y, u, d_{umd}, d_{md} denote the sequences of vectors representing the deviation variable values of the process state of zonal temperature x_T and concentration x_C, the controlled output, the manipulated input which consists of the valve openings and voltage supplied to the fans, the unmeasurable disturbances of animal heat and carbon dioxide generation, the measurable disturbances as the wind speed, wind direction, ambient temperature and concentration level. The representation of these vectors is shown in (14)

$$x = \begin{bmatrix} \bar{T}_1 & \bar{T}_2 & \bar{T}_3 & \bar{C}_{r,1} & \bar{C}_{r,2} & \bar{C}_{r,3} \end{bmatrix}^T_{6\times1}, \quad (14a)$$
$$u = \begin{bmatrix} \bar{A}_{in,i=1\ldots6} & \bar{V}_{volt,j=1\ldots3} \end{bmatrix}^T_{9\times1}, \quad (14b)$$
$$d_{umd} = \begin{bmatrix} \bar{\dot{Q}}_1 & \bar{\dot{Q}}_2 & \bar{\dot{Q}}_3 & \bar{G}_1 & \bar{G}_2 & \bar{G}_3 \end{bmatrix}^T_{6\times1}, \quad (14c)$$
$$d_{md} = \begin{bmatrix} \bar{V}_{ref} & \bar{c}_{P,w} & \bar{c}_{P,l} & \bar{c}_{P,r} & \bar{T}_o & \bar{C}_{r,o} \end{bmatrix}_{6\times1}. \quad (14d)$$

Concluded from systematical analysis, the pair (A,B) is controllable, the pair (C,A) is observable, and the plant is stable. Thus, the model transformation is accomplished and well prepared for solving of the optimization problem in the predictive control scheme which will be discussed in the next section.

B. Disturbance Model and State Estimation

To achieve offset-free control of the output to their desired targets at steady state, in the presence of plant/model mismatch and/or unmeasured disturbances, the system model expressed in (12) is augmented with an integrated disturbance model as proposed in [10] and [11]. The animal heat and contaminant generation partly as a result of function of the number of the animals, are measurable. The parts of the stochastic generation process which in reality affected by various factors, assumed to be unmeasured. The resulting augmented system with process noise n_w and measurement

noise n_v is:

$$\tilde{x}(k+1) = \tilde{A}\tilde{x}(k) + \tilde{B}u(k) + \tilde{G}n_w(k), \tag{15a}$$
$$y(k) = \tilde{C}\tilde{x}(k) + n_v(k), \tag{15b}$$
$$n_w(k) \sim \mathrm{N}(0, Q_w(k)), \tag{15c}$$
$$n_v(k) \sim \mathrm{N}(0, R_v(k)), \tag{15d}$$

in which the augmented state and system matrices are defined as follows,

$$\tilde{x}(k) = \begin{bmatrix} x(k) \\ x_{umd}(k) \end{bmatrix}_{12\times 1}, \tilde{A} = \begin{bmatrix} A & B_{dumd}C_{dumd} \\ 0 & A_{dumd} \end{bmatrix}_{12\times 12},$$
$$\tilde{B} = \begin{bmatrix} B \\ 0 \end{bmatrix}_{12\times 9}, \tilde{C} = \begin{bmatrix} C & 0 \end{bmatrix}_{6\times 12}, \tilde{G} = \begin{bmatrix} B_{dmd} & 0 \\ 0 & B_{dumd} \end{bmatrix}_{12\times 12}. \tag{16}$$

The full process state $x \in \mathbb{R}^6$ and unmeasurable disturbance state $x_{umd} \in \mathbb{R}^6$ are estimated from the plant measurement y by means of a steady state Kalman filter. The process and measurement noise n_w and n_v are assumed to be uncorrelated zero-mean Gaussian noise sequences with covariance Q_w and R_v. The measurable deterministic disturbance $d_{md} \in \mathbb{R}^{12}$ is assumed to remain unchanged within the prediction horizon and equal to the constant at the last measured value, namely $d_{dmd}(k) = d_{dmd}(k+1/k) = \cdots = d_{dmd}(k+H_p-1/k)$. The detectability of the augmented system in 15 is guaranteed when the following condition holds:

$$Rank\begin{bmatrix} (I-A) & -G \\ C & 0 \end{bmatrix} = n + s_d, \tag{17}$$

in which, n is the number of the process states, s_d is the number of the augmented disturbance states. This condition ensures a well-posed target tracking problem. For detailed explanation about the proof refer to [12] and [13].

C. Target Calculation

We now formulate the target tracking optimization as the quadratic program formulation in (18), subjected to the constraints in (19), in which the steady state target of input and state vector u_s and x_s can be determined from the solution of the following computation when tracking a nonzero target vector y_t. The objective of the target calculation is to find the feasible triple (y_s, x_s, u_s) such that y_s and u_s are as close as possible to y_t and u_t, where u_t is the desired value of the input vector at steady state, and, $y_s = Cx_s$.

$$\min_{[x_s,u_s]^T} \Psi = (u_s - u_t)^T R_s (u_s - u_t) \tag{18}$$

$$s.t. \begin{cases} \begin{bmatrix} I-A & -B \\ C & 0 \end{bmatrix}\begin{bmatrix} x_s \\ u_s \end{bmatrix} = \begin{bmatrix} B_{dumd}\hat{d}_{umd,k/k} + B_{dmd}d_{md} \\ y_t \end{bmatrix} \\ u_{\min} \le u_s \le u_{\max} \end{cases}. \tag{19}$$

In this quadratic program, $R_s \in \mathbb{R}^{9\times 9}$ is a positive definite weighting matrix for the deviation of the input vector from u_t. $\hat{d}_{umd,k/k}$ is the current estimate of the unmeasured state disturbance. The equality constraints in (19) guarantee a steady-state solution and offset free tracking of the target vector.

D. Constrained Receding Horizon Regulation

Given the calculated steady state, the constrained optimization problem is formulated by a quadratic cost function (20) on finite horizon, subjected to the following linear equality and inequalities (21) formed by the system dynamics (12) and constraints on the controlled and manipulated variables.

$$\min_{u^N} \Phi_k = \hat{w}_{k+N}^T \bar{Q}_N \hat{w}_{k+N} + \Delta v_{k+N}^T S_N \Delta v_{k+N} + \tag{20}$$
$$+ \sum_{j=0}^{N-1} \left[\hat{w}_{k+j}^T C^T Q C \hat{w}_{k+j} + v_{k+j}^T R v_{k+j} + \Delta v_{k+j}^T S \Delta v_{k+j} \right]$$

$$s.t. \begin{cases} w_{k+j} = x_{k+j} - x_s, \\ v_{k+j} = u_{k+j} - u_s, \\ w_{k+j+1} = Aw_{k+j} + Bv_{k+j}, \\ y_{\min} - y_s \le Cw_{k+j} \le y_{\max} - y_s, j = 1,2,\cdots N \\ u_{\min} - u_s \le v_{k+j} \le u_{\max} - u_s, j = 0,1,\cdots N-1 \\ \Delta u_{\min} \le \Delta v_{k+j} \le \Delta u_{\max}, j = 0,1,\cdots N \end{cases}. \tag{21}$$

where, Φ is the performance index to be minimized by penalizing the deviations of the predictive state $\hat{x}_{k+j}$, control input u_{k+j} and the rate of change Δu_{k+j}, at time j, from the desired steady states. $Q \in \mathbb{R}^{6\times 6}$ and $S \in \mathbb{R}^{9\times 9}$ are symmetric positive semi-definite penalty matrices for process states and rate of input change, $R \in \mathbb{R}^{9\times 9}$ is a symmetric positive definite penalty matrix. It is commonly taken that Q comprises terms of the form C^TC where $r_{k+j} - y_{k+j} = C(x_s - x_{k+j})$. The vector u^N contains the N future open-loop control moves as shown below

$$u^N = \begin{bmatrix} u_k \\ u_{k+1} \\ \vdots \\ u_{k+N-1} \end{bmatrix}. \tag{22}$$

At time $k+N$, the input vector u_{k+j} is set to zero and kept at this value for all $j \ge N$ in the open-loop objective function value calculation. As discussed in the previous section, the plant is stable, therefore, according to [14], Q_N is defined as the infinite sum: $Q_N = \sum_{i=0}^{\infty} A^{T^i} Q A^i$, which will be determined from the solution of the discrete Lyapunov equation: $Q_N = C^TQC + A^TQ_NA$. This regulator formulation guarantees nominal stability for all choices of tuning parameters satisfying the conditions outlined above [15], [16].

The output constraints are applied from time $k+j_1$, $j_1 \ge 1$, through time $k+j_2$, $j_2 \ge j_1$. The value of j_2 is chosen such that feasibility of the output constraints up to time $k+j_2$ implies feasibility of these constraints on the infinite horizon. The value of j_1 is chosen such that the output constraints are feasible at time k. The constrained regulator will remove the output constraints at the beginning of the horizon up to time $k+j_1$ in order to obtain feasible constraints and a solution to the quadratic program. Muske and Rawlings in [15] and [17] explain the existence of finite values for both j_1 and j_2.

Through on-line constrained dynamic optimization, we could obtain a sequence of optimal control signals u^N through a state and disturbance estimator, and the first input value in u^N, u_k, is injected into the plant. This procedure is

repeated by using the plant measurements to update the state vector at time k.

IV. SIMULATION RESULTS

In order to demonstrate the high potential of MPC for multi-objective control within constraints, the comparison between the system behaviors performed with and without controller, in the presence of disturbances and noises, are presented. For the following scenario, we assume that the constraint stability of the control system is guaranteed in the infinite horizon when the feasibility of the input constraints is satisfied within the finite horizon N.

Fig. 3 is derived based on the nonlinear plant model simulation which is developed from a laboratory livestock stable, where the inlet vent opening is limited within $0(m^2)$-$0.6(m^2)$, the supplied voltage to the fan is limited within $0(V)$-$10(V)$, the entire volume of the laboratory livestock stable is around 2500 (m^3). Because of the slow response of the nonlinear system behavior, the sampling time step is defined to be 2 (min), the prediction horizon is $N = 20$. The slew rate of the actuators are very fast compared with the sample time and could be ignored. For animal thermal comfort, the indoor temperature is limited within $\pm 1.5(^oC)$ around the reference value 21^oC within the TNZ. For indoor air quality, the indoor air concentration level should be maintained below $700(ppm)$.

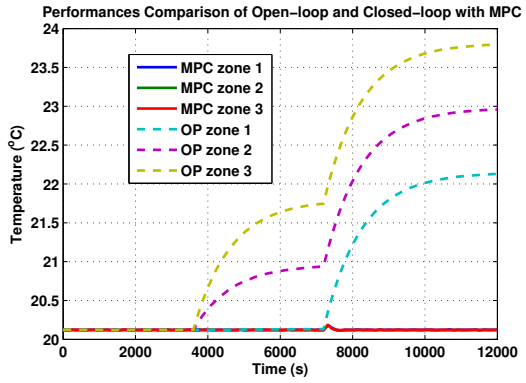

Fig. 3. Rejection of Deterministic Disturbance. Dynamic Performances of Zonal Temperature with and without MPC

The open-loop performing curves (dashed lines) in Fig. 3 demonstrates the thermal system dynamic performances with fixed reference control inputs to the nonlinear system, and clarifies how the imposed disturbances (step changes of ambient weather condition, such as the mean value of external temperature increase from 10 ^oC to 14 ^oC, and pulse changes of heating load, for instance, adding 2000 J/s in the middle zone, and adding 1000 J/s in one of the other two zones) influence the system.

The closed loop performance curves (solid lines) illustrates the results with updated optimum control inputs to the nonlinear thermal comfort system. The weights Q on the tracking errors are different according to different requirement of control objective, the weights R on control inputs and weights S on rate of input change are different for inlets and exhaust fans. Through comparing the simulation results, we could recognize that with the application of MPC, the system behavior has been profoundly modified, and the variance of the output has been reduced considerably.

In the same condition of disturbances setting, but with a step change of the reference value for comfortable temperature, Fig. 4 and 5 show the system performances and actuators behavior. The indoor zonal temperatures keep tracking the reference with slight variations, the carbon dioxide concentration level falls down when the system begin to reject the increase of external temperature by controlling the rotating speed of the fans and opening area of the inlet vents. Thus, the off-set free tracking performances has been achieved by optimizing the steady state value and introducing unmeasurable input disturbance model in terms of integrated white noise. As shown in 5, the voltages of the fans are immediately raised in response to the onset of the disturbance, and ranged against the constraint, hold the value below the constraint while the disturbance is present, and decreased when the disturbance ceases. The variation of the inlet vents openings on the windward side is smaller than the openings on the leeward side, so that the essential negative internal pressure ventilation strategy is always guaranteed, and the wind gust through the inlet can also be avoided. The advantage of MPC handling constraints in a natural and flexible way, is manifested through this example.

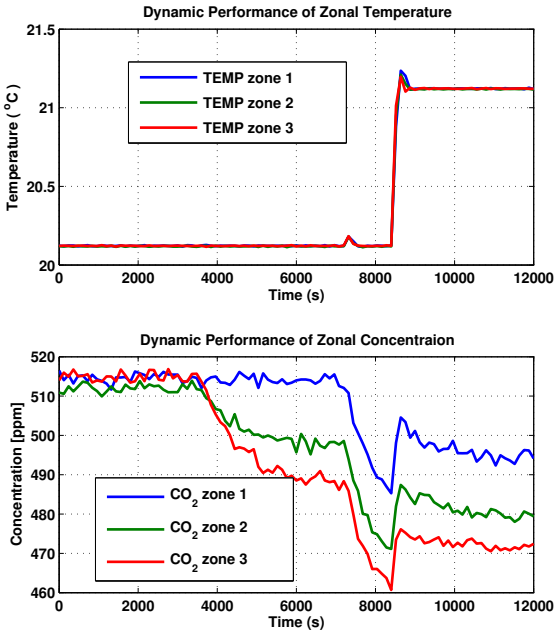

Fig. 4. Reference Tracking and Rejection of Deterministic Disturbance. Dynamic Performances of Zonal Temperature and Concentration

Through step response analysis and bode plot comparison, we realize that, the plant nonlinearities are not highly significant. By varying the disturbances such as the zonal heat sources which cause the direction change of the inter zonal airflow, and varying the external temperature which

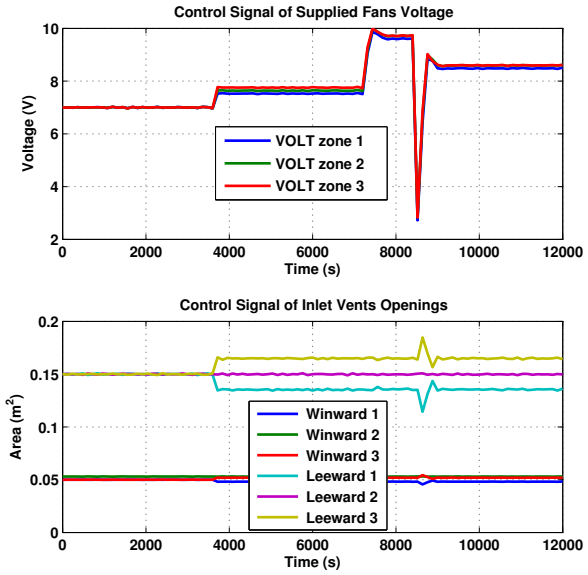

Fig. 5. Optimal Control Signal of Supplied Fans Voltage and Inlet Vents Opening Area

are the leading factors of the variation of the indoor thermal comfort, we obtain similar system behaviors with a series of LTI models.

V. CONCLUSIONS AND FUTURE WORK

A. Conclusions

Aiming at improvement of performances and optimization of energy, the main achievement of this work is the efficient application of MPC for indoor thermal comfort and air quality. In this paper, an LTI model in terms of state space representation which combined the thermal system and concentration system in connection with the air distribution system is derived. The Offset-free control is achieved through target calculation, quadratic programming and augmentation with unmeasured input disturbance model. The presented simulation results show the significant advantages of using MPC over linear models for control.

B. Future Work

The Moving Horizon Estimation method will be applied when the unmeasured disturbance constraints are presented and further performance improvement are needed. The weighting matrix on the states of indoor temperature and concentration will be further adjusted in order to achieve a better equilibrium between multiple objectives requirements. The entire control system will be identified through experiments in a real scale livestock barn equipped with hybrid ventilation systems in Syvsten, Denmark, and the result will be compared with those obtained with the currently used controller.

VI. ACKNOWLEDGMENTS

The authors gratefully acknowledge the contribution and financial support from the Danish Ministry of Science and Technology (DMST), and Center for Model Based Control (CMBC) under Grant: 2002-603/4001-93.

REFERENCES

[1] P. Heiselberg, Principles of Hybrid Ventilation, *IEA Energy Conservation in Buildings and Community Systems Program, Annex 35: Hybrid Ventilation in New and Retrofitted Office Building*, Aalborg, Denmark, 2002.

[2] J. M. Maciejowski, *Predictive Control with Constraints*, Prentice Hall, England; 2002.

[3] J. A. Rossiter, *Model-based Predictive Control, A Practical Approach*, CRC Press, Boca Raton, Florida; 2003.

[4] D. Q. Mayne, J. B. Rawlings, C. V. Rao, P. O. M. Scokaert, Constrained model predictive control: Stability and optimality, *Automatica*, vol. 36, 2000, pp. 789 - 814.

[5] G. Pannocchia, N. Laachi, J. B. Rawlings, A Candidate to Replace PID Control: SISO-Constrained LQ Control, *AIChE J.*, vol. 51, 2005, pp. 1178-1189.

[6] S. J. Qin, T. A. Badgwell, "An overview of industrial model predictive control technology", *in fifth International Conference on Chemical Process Control, AIChE Symposium Series*, Vol. 93, No. 316, 1997, pp. 232 - 256.

[7] Z. Wu, P. Heiselberg, J. Stoustrup, "Modeling and Control of Livestock Ventilation Systems and Indoor Environments", *in 26th AIVC Conference on Ventilation in Relation to the Energy Performance of buildings*, Brussels, Belgium, 2005, pp. 335-340.

[8] W. Van der Hel, R. Duijghuisen, M. W. A. Verstegen, The effect of ambient temperature and activity on the daily variation in heat production of growing pigs kept in groups, *J.Agric. Sci.*, vol. 34, 1986, pp. 173 - 184.

[9] R. Geers, H. Ville, V. Goedseels, Environmental temperature control by the pig's comfort behavior through image processing, *Trans. ASAE*, vol. 34, No. 6, 1991, pp. 2583 - 2586.

[10] G. Pannocchia, J. B. Rawlings, Disturbance models for offset-free model predictive control, *AIChE J.*, vol. 49, No. 2, 2003, pp. 426-437.

[11] K. R. Muske, T. A. Badgwell, Disturbance modeling for offset-free linear model predictive control, *Journal of Process Control*, vol. 12, 2002, pp. 617-632.

[12] J. B. Rawlings, Tutorial Overview of Model Predictive Control, *IEEE Control Systems Magazine*, 2000.

[13] C .V. Rao, J. B. Rawlings, Steady States and Constraints in Model Predictive Control, *AIChE J.*, Vol. 45, No. 6, 1999, pp. 1266 - 1278.

[14] K. R. Muske and J. B. Rawlings, Model Predictive Control with Linear Models, *AIChE J.*, vol. 39, No. 2, 1993, pp. 262 - 287.

[15] K. R. Muske, J. B. Rawlings, Linear Model Predictive Control of Unstable Processes, *Journal of Process Control*, vol. 3, No. 2, 1993, pp. 85 - 96.

[16] D. Q. Mayne, J. B. Rawlings, C. V. Rao, P. O. M. Scokaert, Constrained model predictive control: Stability and optimality, *Automatica*, vol. 36, 2000, pp. 789 - 814.

[17] K. R. Muske, Linear Model Predictive Control of Chemical Process, *Ph.D. Thesis*, The University of Texas at Austin, 1995.